AD 268 360

THE ANTENNA LABORATORY

RESEARCH ACTIVITIES in ---

Automatic Controls — *Antennas* — *Echo Area Studies*
Microwave Circuits — *Astronautics* — *E M Field Theory*
Terrain Investigations — *Radomes* — *Systems Analysis*
Wave Propagation — *Submillimeter Applications*

A Systematic Method for Character Recognition

by

David L. Fritzsche

Contract AF 33 (616) - 6137
Task No. 50682

1222-4 15 Nov. 1961

Department of ELECTRICAL ENGINEERING

THE OHIO STATE UNIVERSITY
RESEARCH FOUNDATION
Columbus, Ohio

REPORT 1222-4

REPORT

by

THE OHIO STATE UNIVERSITY RESEARCH FOUNDATION

COLUMBUS 12, OHIO

Cooperator	Aeronautical Systems Division Air Force Systems Command United States Air Force Wright-Patterson Air Force Base, Ohio
Contract	AF 33 (616) - 6137
Task Number	50682
Investigation of	Guidance and Sensing Techniques for Advanced Vehicles.
Subject of Report	A Systematic Method for Character Recognition
Submitted by	David L. Fritzsche Antenna Laboratory Department of Electrical Engineering
Date	15 November 1961

ACKNOWLEDGEMENTS

The author wishes to express his sincere appreciation to Prof. R. L. Cosgriff for his aid and suggestions in the development of this report.

CONTENTS

	Page
CHAPTER I	
INTRODUCTION	1
CHAPTER II	
REPRESENTATION OF CHARACTERS	4
CHAPTER III	
COMPARISON OF CHARACTERS	
A. Method of Comparison	9
B. Preliminary Adjustments	12
C. Absolute Upper Bound	15
D. Sample Characters	16
E. Tabulated Error and Discussion of Results	17
CHAPTER IV	
CONCLUSIONS	22
APPENDIX I	
TABULATION OF $G(\ell_1)$	24
APPENDIX II	
TESTING OF DIGITAL COMPUTER RESULTS	77
BIBLIOGRAPHY	81

CHAPTER I

INTRODUCTION

The rapid expansion of digital computer usage has created the need for a means of transmitting written data directly to the computer without the manual translation such as that commonly performed by card punch operators. A satisfactory system which will accept written data and translate these data to machine language would have numerous applications in addition to those in the computer field. Automatic sorting of mail, office automation, and machine translation of written material from one language to other languages are some of the applications that come to mind. At the present time, most methods [1,2,3] * for automatic recognition of written data have been restricted to use of a carefully selected format for a group of written symbols.

A paper, [4] "Pattern Detection and Recognition", by S. H. Unger presents a method which does not limit character size and style severely. The method suggested and tested requires the superimposing of line type patterns on a grid. All grid squares through which a line passes are tabulated. This information is processed by a computer. The computer answers a series of questions, such as , "Does the pattern consist of straight lines only ? ", "Does the pattern contain arcs opening to the

---

* All references are listed in the bibliography.

left?","Does the pattern contain arcs opening to the right ?", etc. By the process of elimination, the pattern is identified providing the data for the pattern are stored in the computer memory.

The report,[5] "Identification of Shape," by R. L. Cosgriff demonstrates that shapes can be uniquely represented by a continuous periodic function. The function can be represented by a number of the orthogonal sets. This method of representation and a technique for recognition is developed and extended in this paper.

A second method which uniquely describes a character is a curve of R versus θ, Fig. 1-1. This method can be used only with the simple characters since multiple values of the $R(\theta)$ function occur with complex characters. Also, this representation has the disadvantage of being dependent upon the origin location.

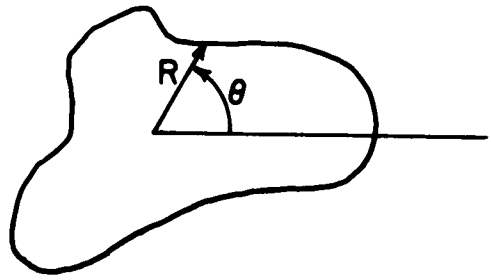

Fig. 1.1. Geometrical description of R vs. θ representation method.

In the discussion of mathematical techniques for symbol recognition, it is necessary to remember that the nature of the selectivity

(ability to distinguish two dissimilar symbols) will be dependent upon the techniques involved. Furthermore, we should not expect an exact correpondence between selectivity of any mathematical technique and the selectivity of the human. Notice the characters in Fig. 1-2 and see the similarities as you progress from a to b to c. Yet these same characters, if rotated 90^{o}, form the letters H, K, and X. H, K, and X each has a definite but different meaning. The human is conditioned to observe the differences rather than the very pronounced similarities of these three letters. We can not expect a mathematical comparison of characters to indicate to the same degree those differences or similarities which we observe.

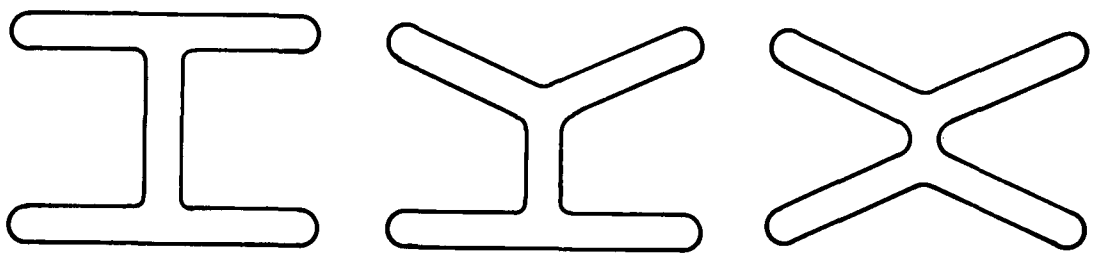

Fig. 1.2. Simple similar characters with different meanings.

CHAPTER II

REPRESENTATION OF CHARACTERS

Characters or figures can be classified in many ways. In this paper, a character or figure will be considered to be simple if it can be defined by a single closed curve. If the figure can not be defined by a single closed curve, the figure will be considered complex. Complex figures require a finite number of closed curves or shade variation for satisfactory description. Many figures are composed of a group of lines with finite width. If the outside boundry of such figures can be used to define the figure the figure is said to be reducible to simple form. For example, all printed letters which can be represented by intersecting lines which do not enclose an area or areas are reducible to simple form. On the other hand, the letters B, P, etc. cannot be reduced to simple form without altering the figure. However, some such letters or figures may be easily recognized by the outside boundry alone. Techniques for representing or approximating complex figures can be developed but will not be considered. Only simple figures or characters will be considered.

Two basic characteristics of simple figures are employed in the development of a mathematical representation. The first variable is arc length.

$$(1) \qquad L = \oint_C d\ell$$

where L is the total length and $d\ell$ is the incremented arc length of the line which defines the figure. A suitable technique for figure recognition is not dependent upon the line length L. Therefore, normalizing the total line length of all characters to 2π will eliminate possible restrictions on character size and will be convenient in further development of a mathematical representation. The normalized length ℓ_1 is such that

$$(2) \qquad L_1 = \oint_{C_1} d\ell_1 = \frac{2\pi}{L} \oint d\ell = 2\pi$$

Consider the second characteristic of a simple figure. If the figure is composed of straight lines only, then the sum of the exterior angles ϕ_{e_n} is :

$$(3) \qquad \sum_{h=1}^{N} \phi_{e_n} = 2\pi$$

providing the defining lines are traversed only once. If the lines are traversed m times then

$$(4) \qquad \sum_{h=1}^{N} m\, \phi_{e_n} = 2m\pi$$

If the straight line segments of the figure are joined by curves, then Eq. (4) can be expressed in integral form .

$$(5) \qquad 2m\pi = \oint \frac{d\phi}{d\ell}\, d\ell$$

where $\frac{d\phi}{d\ell}$ at any given point is equal to $1/r_c$, with r_c the radius of curvature, m the number of times the figure is traversed, and ϕ the angle the tangent to the curve makes relative to some arbitrary reference line in the plane of the figure.

The two fundamental characteristics of simple figures allows all such figures to be represented graphically. A plot of the tangent angle versus ℓ is a unique representation. The tangent angle is measured with respect to some arbitrary reference in the plane of the figure. The figures are represented by

$$\phi = F(\ell_1) \tag{6}$$

after the normalization of ℓ. The second characteristic considered above indicates that $F(\ell_1)$ is a curve of ever increasing value if the figure is traversed m times. However, $F(\ell_1)$ is always equal to mL_1 after traversing the figure m times. The curve can be made periodic by subtracting the ramp function $\phi = \ell_1$ from Eq. (4) giving

$$\phi - \ell_1 = G(\ell_1) \tag{7}$$

A simple figure can be uniquely represented by the function $G(\ell_1)$. $G(\ell_1)$ is a piecewise continuous, bounded, and periodic function and can be represented by a Fourier series.

$$G(\ell_1) = a_o + \sum_{n=1}^{\infty} (a_n \cos n\ell_1 + b_n \sin n\ell_1) \tag{8}$$

The constant a_o can be eliminated by choosing the reference angle properly and will be neglected.

Figure 2-1 illustrates the technique for representing any simple curve as some function $G(\ell_1)$. Figure 2-1a is a sketch of a simple character with an indicated starting point. (The line is traversed in the counterclockwise direction.) An arbitrary reference angle and the tangent to the curve at a given point are also shown. This figure has been chosen to test the performance of computer programming and accuracy because the Fourier series for $G(\ell_1)$, as shown in Fig. 2-1c, can be readily calculated. Appendix Table A-35 shows the computer results and calculated results for Fig. 2-1a.

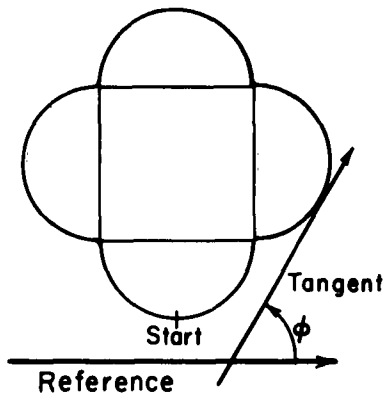

a) Sketch of a simple character.

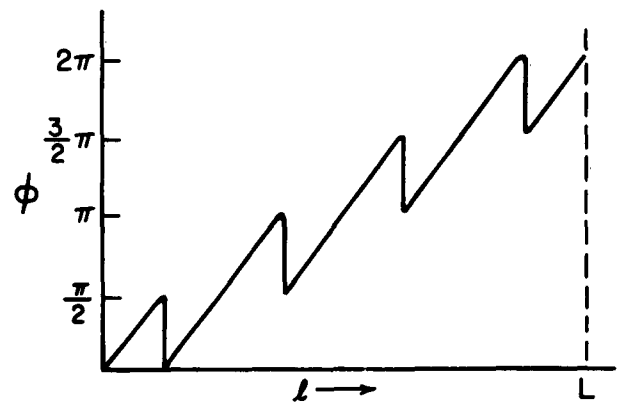

b) The ϕ vs. ℓ curve for this character.

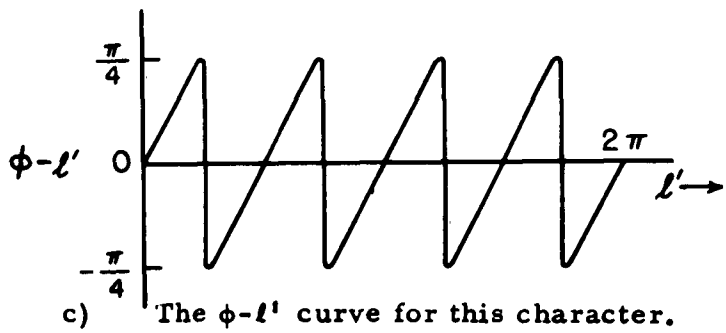

c) The ϕ-ℓ' curve for this character.

Fig. 2.1

CHAPTER III

COMPARISON OF CHARACTERS

A. Method of Comparison

In the last chapter it was demonstrated that any given simple figure can be represented by a Fourier series. This series can be reduced to:

$$(9) \qquad G(\ell_1) = \sum_{n=1}^{\infty} C_n \cos (n \ell_1 - \theta_n)$$

where the constant a_o has been neglected for reasons previously indicated.

In this chapter, a technique will be developed for specifying an arbitrary character as being identical or similar to one of a group of P standard characters. Each of the P characters can be represented as $G_p(\ell_1)$ for $1 \leq p \leq P$. The arbitrary character is represented as $G_q(\ell_1)$.

Because of the orthogonality of the Fourier series, it is convenient to express the degree of similarity between $G_q(\ell_1)$ and $G_p(\ell_1)$ as a mean square error E_{pq}.

$$(10) \qquad E_{pq} = \frac{1}{2\pi} \int_0^{2\pi} |G_p(\ell_1) - G_q(\ell_1)|^2 \, d\ell_1$$

$$= \frac{1}{2\pi} \sum_{n=1}^{\infty} \int_0^{2\pi} |C_{np} \cos (n\ell_1 - \theta_{np}) - C_{nq} \cos (n\ell_1 - \theta_{nq})|^2 d\ell_1$$

(10) (Cont.)
$$= \tfrac{1}{2} \sum_{n=1}^{\infty} \left[(C_{np})^2 + (C_{nq})^2 - 2C_{np} C_{nq} \cos \alpha_n \right]$$

where $\alpha_n = \theta_{nq} - \theta_{np}$. Practical considerations require limiting the summation to N terms such that :

(11)
$$G(\ell_1) \cong \sum_{n=1}^{N} C_n \cos (n\ell_1 - \theta_n)$$

and

(12)
$$E_{pq} \cong \tfrac{1}{2} \sum_{n=1}^{N} \left[(C_{np})^2 + (C_{nq})^2 - 2 C_{np} C_{nq} \cos \alpha_n \right]$$

Before continuing further along this line of thought, it clarifies the problem if each $G_p(\ell_1)$ is represented in 2N dimensional vector space. The unit vectors in 2N dimensional space are

$$\vec{r}_n \text{ and } \vec{i}_n \qquad\qquad n = 1, 2, 3, \ldots N.$$

Since

$$G_p(\ell_1) = \sum_{n=1}^{N} C_{np} \cos (n\ell_1 - \theta_{np})$$

$$= \sum_{n=1}^{N} a_{np} \cos n\ell_1 + b_{np} \sin n\ell_1$$

then $G_p(\ell_1)$ can be represented as a unique point in 2N vector space. The

vector from the origin to the point P is:

$$(13) \qquad \overrightarrow{OP} = \sum_{n=1}^{N} \left[\vec{r}_n \, a_{np} + \vec{i}_n \, b_{np} \right]$$

$$= \sum_{n=1}^{N} \left[\overrightarrow{a_{np}} + \overrightarrow{b_{np}} \right]$$

where $|\overrightarrow{a_{np}}|$ and $|\overrightarrow{b_{np}}|$ are in the $\vec{r}_n$ and $\vec{i}_n$ directions, respectively. The character $G_q(\ell_1)$ can be represented in like manner, so that:

$$(14) \qquad G_q(\ell_1) = \sum_{n=1}^{N} \left[\overrightarrow{a_{nq}} + \overrightarrow{b_{nq}} \right]$$

It follows that the vector $\overrightarrow{PQ}$ is a measure of the similarity of $G_p(\ell_1)$ and $G_q(\ell_1)$, because if, $G_p(\ell_1) = G_q(\ell_1)$ then $\overrightarrow{PQ} = 0$.

$$(15) \qquad \overrightarrow{PQ} = \sum_{n=1}^{N} \left[\overrightarrow{a_{nq}} + \overrightarrow{b_{nq}} - \overrightarrow{a_{np}} - \overrightarrow{b_{np}} \right]$$

$$= \sum_{n=1}^{N} \left[\overrightarrow{C_{nq}} - \overrightarrow{C_{np}} \right]$$

where $|\overrightarrow{C_n}| = (a_n^2 + b_n^2)^{\frac{1}{2}}$.

The absolute magnitude squared of the vector $\overrightarrow{PQ}$ is identical to twice the mean squared error as determined by Eq. (12).

$$(16) \qquad |PQ|^2 = E_{pq} = 2 E_{pq} .$$

Henceforth, the error E_{pq} shall be used to designated the degree of similarity between the p^{th} and q^{th} figures.

B. Preliminary Adjustments

The function $G(\ell_1)$, Eq. (7), is dependent upon the origin of $F(\ell_1)$, (Eq. (6)). Also, $F(\ell_1)$ is dependent upon the starting point for traversing the defining curve of a simple figure. It logically follows that the vector $\overrightarrow{PQ}$ is dependent upon the origin of $F_p(\ell_1)$ and $F_q(\ell_1)$. In order to use the error E_{pq} as a true indication of similarity, it must be minimized to its least possible value.

Allow the vector representation of $G_p(\ell_1)$, $\overrightarrow{OP}$, to remain fixed in vector space. Allow the vector representing $G_g(\ell_1)$ to describe some closed contour in 2N dimensional vector space. This closed contour is generated by shifting the origin of $G_q(\ell_1)$ from 0 to 2π. This shifting operation necessitates rewriting the expression for $G_q(\ell_1)$, $\overrightarrow{OQ}$, as

$$(16) \qquad \overrightarrow{OQ} = \sum_{n=1}^{N} \overrightarrow{C_{nq} \cos(\theta_{nq} + n\beta)} + \overrightarrow{C_{nq} \sin(\theta_{nq} + n\beta)}$$

Then the vector difference

$$(17) \qquad \overrightarrow{PQ} = \sum_{n=1}^{N} \left[\overrightarrow{a_{np}} + \overrightarrow{b_{np}} - \left(C_{nq} \overrightarrow{\cos(\theta_{nq} + n\beta)} + C_{nq} \overrightarrow{\sin(\theta_{nq} + n\beta)} \right) \right]$$

$$= \sum_{n=1}^{N} \left[\overrightarrow{C_{np}} - \overrightarrow{C_{nq}} \right]$$

where $|\overrightarrow{C_{np}}|$ and $|\overrightarrow{C_{nq}}|$ have the same definition as previously indicated. Then the error E_{pq} is :

$$(18) \qquad E_{pq} = |PQ|^2 = \sum_{n=1}^{N} \left[(C_{np})^2 + (C_{nq})^2 - 2C_{np}C_{nq} \cos(\alpha_n + n\beta) \right]$$

where $\alpha_n = \theta_{nq} - \theta_{np}$. The maximization of the last term on the right side of Eq. (18) results in a minimization of E_{pq} . The minimum E_{pq} results with a proper choice of β. This choice of β is most readily determined with a digital computer if the q^{th} figure is to be compared with P standard figures. A graphical solution for β is possible although it is a lengthy and tedious process.

It has been shown that the starting point on the line defining a simple figure is arbitrary for the determination of $G(\ell_1)$. However, the starting point must be adjusted mathematically if the minimum value of E_{pq} is to be calculated. This corresponds to using a common starting point for identical figures. If two figures are identical, then a common starting point is determined by

$$(20) \qquad \theta_{1q} - \theta_{1p} + \beta = 0$$

where the phase of the p^{th} figure remains fixed.

Now consider the case where C_{1q} of $G_q(\ell_1)$ is zero. θ_{1q} can assume any arbitrary value between 0 and 2π. The solution of β in Eq. (20) is not unique and a common starting point can not be found in this

manner. In general, the same argument holds if $C_{1q} \ll C_{nq}$, such that small errors in the calculation of C_{1q} result in large errors in θ_{1q}. The solution for β in Eq. (20) is possible for the general case but is not sufficiently accurate.

A second method for determining an approximate minimum value of **E** is to locate the largest product $2C_{np}C_{nq}$ in the summation

$$\sum_{n=1}^{N} 2\, C_{np}C_{nq} \cos\,(\alpha + n\beta).$$

Then $\cos\,(\alpha_n + n\beta)$ for this term is set equal to one. This method assumes that the n^{th} term of the p^{th} and q^{th} figures are larger than all other terms. This assumption is valid if only figures with a high degree of similarity are of interest. In order to systemmatize this method, the starting points for each $G_p(\ell_1)$ and $G_q(\ell_1)$ are adjusted such that θ_{np} and θ_{jq} are zero, where θ_{np} and θ_{jq} are the phases of the largest term in each series. The error E_{pq} calculated in this manner will approach its minimum value for similar figures but will not necessarily approach the minimum value for dissimilar figures. One discrepancy may arise with the use of this technique if C_j and C_{j+k} are of nearly equal magnitudes. Which of these two terms should be phased to zero ? This question can be reconciled by computing the error E_{pq} twice, once with $\theta_j + \beta_j = 0$ and once with $\theta_{j+k} + \beta_{j+k} = 0$. The lesser value of E_{pq}

will be the more accurate indication of similarity.

For this paper, the starting point on each describing curve is first chosen by visual inspection such that E_{pq} approximates its minimum possible value. The approximation is improved in accuracy by adjusting the phase of the largest term of each $G(\ell_1)$ to zero. This corresponds to small adjustments of the starting points.

C. Absolute Upper Bound

The method to be used for determining the approximate minimum value of E_{pq} can be checked for accuracy as follows. The absolute minimum value of E_{pq} is :

$$(21) \qquad (E_{pq})_{min} = \sum_{n=1}^{N} |C_{np} - C_{nq}|^2$$

which assumes all terms of $G_p(\ell_1)$ and $G_q(\ell_1)$ are in phase. For similar figures, this value of $(E_{pq})_{min}$ will be approached. If the calculated value of E_{pq} does not approach $(E_{pq})_{min}$ then this indicates either that the starting points have been chosen improperly or that the figures are dissimilar. The calculation of $(E_{pq})_{min}$ can be used as a rapid and convenient indication of the degree of similarity. A large value of $(E_{pq})_{min}$ immediately shows dissimilarity. On the other hand, a small value of $(E_{pq})_{min}$ does not necessarily show a high degree of similarity. The upper bound $(E_{pq})_{min}$ establishes one level of similarity.

A second level is established by some upper allowable limit to E_{pq}. This second level is specified according to the purpose of the identification system when employed as in $(E_{pq})_{min}$.

D. Sample Characters

The figures shown on the Appendix I of this paper (Figs. A-1 through A-34) represent a sample of the figures which can be identified using the technique previously described. The series $G(\ell_1)$ which represents each character are tabulated in the Appendix I. The figures and corresponding tables have identical numbers. The amplitudes of each term of the harmonic series have been computed for the first thirty terms and the phase of each term has been adjusted so that θ_n for the largest term is zero.

Most of the characters are letters of the alphabet or are a modification of these characters. These characters have been chosen for their practical value. A second reason for choosing letters is because the series $G(\ell_1)$ exhibit convergence in the first thirty terms. The other characters (animals, faces, etc.) do not converge rapidly in the first thirty terms and are not entirely satisfactory for this initial study. These figures do show the limitations of such a technique.

E. Tabulated Error and Discussion of Results

There are over seven hundred possible comparisons which can be made using the characters referred in the previous section. A visual check of the Fourier series coefficients and phase angles as tabulated in the Appendix I readily shows that $(E_{pq})_{min}$ for characters which appear dissimilar will be quite large (i.e. greater than 0.5). For this reason the majority of the possible comparisons are not carried out.

Forty one comparison have been made and are tabulated in Table 3-1. The first column of the table designates the characters being compared. The second column labeled E_5 is the error obtained by using only the first five terms of each series $G(\ell_1)$. Columns 3, 4 and 5 have similar significance. It will be noted that the columns labeled E_{20} and E_{30} are not complete. A study of those comparisons which are complete will show that two figures which appear similar to the eye will have a small E_{pq} using only five or ten terms of $G(\ell_1)$. Here again a small E_{pq} is assumed to be less than 0.5. This value of E_{pq} and $(E_{pq})_{min}$ has been arrived at after a study of Table 3-1 and the figures presented in Appendix I. A lesser or greater value may be used depending upon the degree or level of similarity desired.

Several of the comparisons in Table 3-1 bear special attention. Note the error E_5 for comparing the X, H, and K on Figs. A-1, A-6 and

TABLE 3-1

TABULATED ERROR

Figure	Compared	E_5	E_{10}	E_{20}	E_{30}
A-1	A-2	0.038	0.074	0.317	0.458
A-1	A-3	0.080	0.160	0.210	0.222
A-1	A-5	2.699	2.927	3.005	3.025
A-1	A-6	0.902	1.079	1.142	1.148
A-1	A-7	0.741	0.886	0.958	0.973
A-1	A-8	2.164	2.260	2.313	2.320
A-1	A-9	2.772	2.828	2.888	2.897
A-1	A-10	1.941	2.087	2.135	2.144
A-1	A-31	3.805	5.450	6.122	6.172
A-1	A-32	4.436	5.510	6.595	6.773
A-2	A-3	0.169	0.261	0.550	0.710
A-3	A-4	0.036	0.096	0.147	0.156
A-3	A-5	2.441	2.893	2.938	2.953
A-6	A-7	0.098	0.168	0.219	0.223
A-8	A-9	2.280	2.470	2.477	2.479
A-8	A-10	0.116	0.151	0.157	0.159
A-8	A-11	1.260	1.347	-	-
A-10	A-11	1.896	2.002	-	-
A-10	A-12	0.690	0.744	-	-
A-13	A-14	2.067	2.569	-	-
A-16	A-17	4.358	4.457	-	-
A-16	A-18	4.595	4.731	-	-
A-17	A-18	6.817	7.029	-	-
A-17	A-23	0.712	0.782	-	-
A-17	A-24	1.645	1.884	-	-
A-18	A-23	6.398	6.518	-	-
A-21	A-21a	0.114	0.147	0.197	0.265
A-21	A-21ab	0.161	0.299	0.388	0.495
A-21	A-21abc	0.166	0.349	0.583	0.675
A-21a	A-21ab	0.049	0.115	0.193	0.232
A-21a	A-21abc	0.378	0.603	0.795	0.885
A-21ab	A-21abc	0.380	0.796	1.170	1.308
A-21	A-22	3.408	3.619	-	-
A-23	A-24	0.495	0.650	-	-
A-23	A-25	1.865	2.048	-	-
A-27	A-28	0.830	1.062	-	-
A-27	A-33	1.852	2.956	-	-
A-30	A-31	2.654	5.447	-	-
A-30	A-32	4.052	7.265	-	-
A-33	A-34	1.853	3.255	-	-
A-32	A-34	2.534	3.244	-	-

A-7 respectively. The error for these comparisons indicates a relatively high degree of similarity although the figures were not drawn for the purpose of showing this similarity. The degree of similarity between Fig. A-1 and A-2 and also Fig. A-3 and A-4 is quite high which is the desirable result.

The errors resulting from all possible comparisons of Fig. A-21, A-21a, A-21ab, and A-21abc require further explanation. These figures have been used as a basis for studying distortion. Distortions as used here refers to the modification of a standard figure in some small way such that the standard figure is still easily recognized visually. Furthermore, the modification effects only some small portion of the standard figure. Using only five terms in the calculation of E_{pq} for the figures indicated results in a satisfactory indication of similarity although not what the human might expect. For example, Fig. A-21abc is expected to compare most favorably with Fig. A-21ab. However, Fig. A-21abc compares most favorably with Fig. A-21. If all thirty terms of $G(\ell_1)$ are used in the comparisons, this discrepancy between the eye and mathematical results is further enhanced.

Small distortions, i.e., the line length which describes the distortion is small compared to the line length of the total standard figure, can be treated as being a linear addition to $G_s(\ell_1)$. $G_s(\ell_1)$ is the function which describes a standard figure. A small distortion which adds a rectangular pulse to $G_s(\ell_1)$ contains frequency components

whose magnitude is proportional to $\sin \pi \ell_2 f / \pi \ell_2 f$, where ℓ_2 is the length of the distortion. Thus, a rectangular pulse adds a significant amount to $G_s(\ell_1)$ over the frequency range up to $f = 1/\ell_2$. A distortion of length ℓ_3 which adds the derivative of a triangular pulse to $G_s(\ell_1)$; adds frequency components of increasing magnitude up to $f = 1/\ell_3$ and can be considered insignificant above $f = 2/\ell_3$. These two examples of possible distortions show the difficulties which arise if distorted figures are considered. Multiple distortions on a given standard figure or increased size of the distortions also modify $G_s(\ell_1)$ to the extent where similarity can not be shown using the described technique. The results obtained from the comparison of Fig. A-33 and A-34 indicates the large error obtained in this case.

The error calculated for the comparison of Fig. A-1 and A-2 shows that the addition of small distortions placed symmetrically on a standard figure may possibly be treated as a linear addition to $G_s(\ell_1)$. The distortions add components primarily to the higher harmonics. This is only one of many possible examples of symmetrical addition and is sufficient for showing general conclusions.

A plot of $(E_{pq})_{min}$ and E_{pq} is shown in Fig. 3-1. This figure uses only the first five terms of $G(\ell_1)$ and demonstrates that starting points have been properly chosen for an approximation of the minimum possible E_{pq}. Those points denoted by open dots are comparisons which

are considered to show a desired level of similarity both visually and mathematically. Those points denoted by closed dots show dissimilarity both mathematically and visually. Not all forty one comparisons have been entered in Fig. 3-1, but a sufficient number are shown to indicate the type of plot which is obtained.

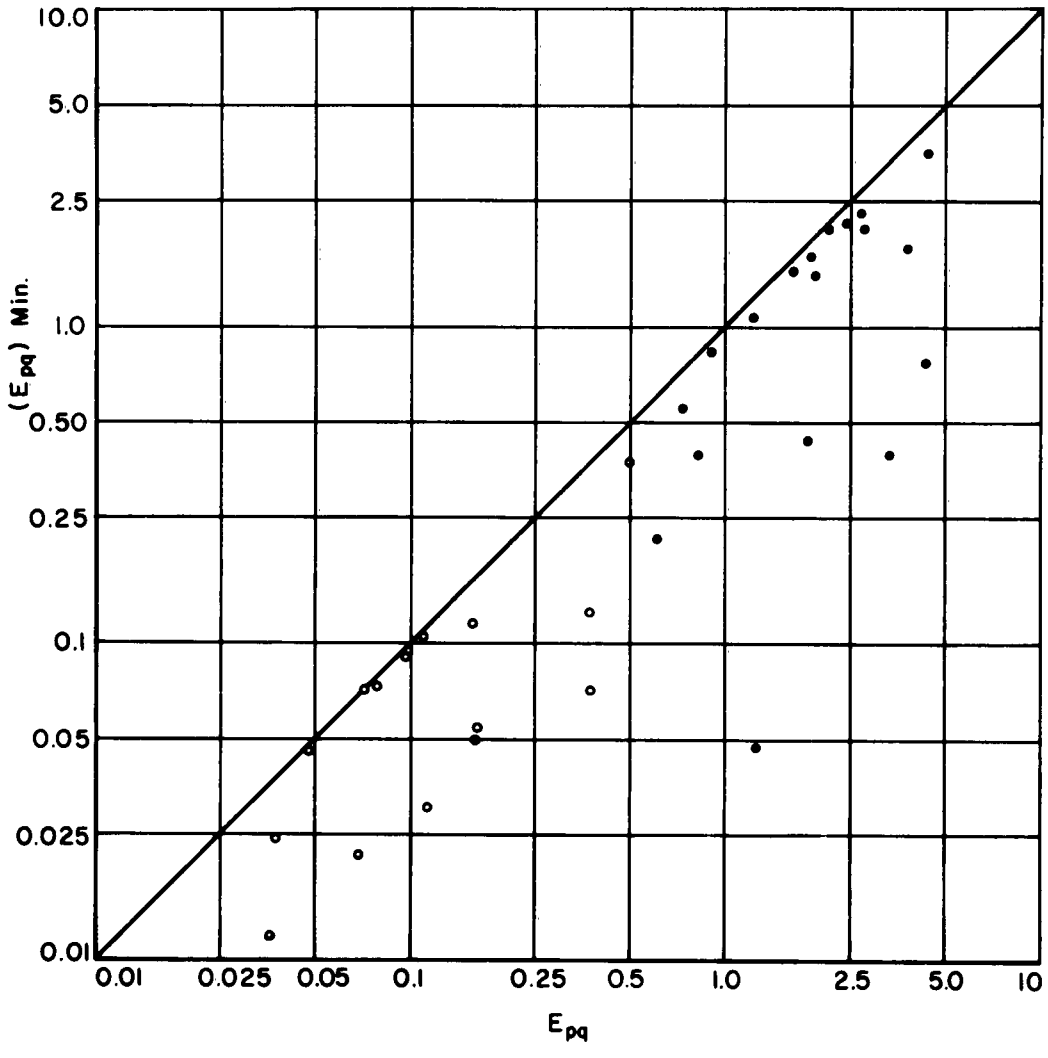

Fig. 3.1. Representative sample of $(E_{pq})_{min}$ vs. E_{pq} for first five terms of G (4).

CHAPTER IV

CONCLUSIONS

A technique which is described for character recognition which has been described possesses several characteristics necessary for satisfactory recognition. Not all of these characteristics are present in many of the methods which have been used for character recognition. The desirable characteristics are :

(1.) Each character is representable by a unique mathematical expression.

(2.) The recognition technique is independent of character size.

(3.) The technique is independent of character orientation, and

(4.) The gross features of a character are identified by using only a limited number of terms of the mathematical expression.

The principal disadvantage of the technique is that it is sensitive to irregularities or distortions of standard figures. This may be considered an advantage if it is known that such distortions represent the difference between two given figures.

The technique as presented is feasible for the recognition of typed letters or numbers, where the figures are distinct and are identical for each appearance. Hand written letters and words are not adaptive to this technique because of the immense number of standard characters which would be necessary.

Earlier methods which were considered for character recognition involved optical matching. The difficulties which arose were due primarily to orientation and size of characters. These problems have been overcome for the method shown by describing each character as a function $G(\ell_1)$. The optical matching of these functions may prove to be more satisfactory than the mathematical matching as described in the paper.

APPENDIX I

TABULATION OF $G(\ell_1)$

[Fourier Cosine Coefficients and Phase Angles]

TABLE A-1

n	C_n (radians)	θ_n (degrees)
1	0.05184	185.3
2	0.03705	41.0
3	0.11825	42.7
4	1.27951	0
5	0.13563	153.2
6	0.20167	206.3
7	0.05685	56.2
8	0.05895	71.9
9	0.00905	208.8
10	0.02379	149.1
11	0.01643	194.6
12	0.09442	177.4
13	0.09248	331.6
14	0.06604	297.0
15	0.06835	280.8
16	0.12990	257.2
17	0.03956	99.4
18	0.05894	124.3
19	0.01255	306.4
20	0.03000	24.8
21	0.05546	121.3
22	0.03013	72.0
23	0.00682	88.4
24	0.01445	68.2
25	0.03206	247.7
26	0.01711	193.1
27	0.01749	203.5
28	0.01473	188.4
29	0.03522	337.4
30	0.01892	327.2

TABLE A-2

n	C_n (radians)	θ_n (degrees)
1	0.10458	204.2
2	0.12810	129.9
3	0.18264	67.7
4	1.36676	0
5	0.16981	113.1
6	0.14460	219.9
7	0.09753	339.2
8	0.00766	60.9
9	0.03449	199.0
10	0.10237	173.0
11	0.10782	72.2
12	0.05419	177.9
13	0.24204	291.3
14	0.30895	224.8
15	0.16405	338.4
16	0.03157	99.0
17	0.20595	204.4
18	0.17925	133.2
19	0.08616	244.5
20	0.09748	357.6
21	0.24765	109.9
22	0.04534	54.8
23	0.03645	330.8
24	0.00868	69.3
25	0.19315	200.0
26	0.02062	122.3
27	0.21652	67.6
28	0.03147	340.6
29	0.09741	112.2
30	0.00701	107.7

TABLE A-3

n	C_n (radians)	θ_n (degrees)
1	0.00460	9.7
2	0.20542	46.4
3	0.01040	309.3
4	1.15341	0
5	0.01073	239.6
6	0.18173	133.9
7	0.01253	32.6
8	0.09364	93.4
9	0.01191	239.0
10	0.15829	228.7
11	0.00634	64.7
12	0.01915	17.0
13	0.00714	247.5
14	0.11545	316.1
15	0.00576	185.3
16	0.01775	276.2
17	0.00362	122.9
18	0.06476	40.2
19	0.00611	324.3
20	0.01460	177.0
21	0.00733	96.1
22	0.04000	156.2
23	0.01157	293.8
24	0.03810	268.9
25	0.00272	121.6
26	0.02238	212.6
27	0.00277	159.1
28	0.02923	22.1
29	0.00059	320.2
30	0.00729	252.1

TABLE A-4

n	C_n (radians)	θ_n (degrees)
1	0.01138	201.4
2	0.11058	46.6
3	0.04152	46.8
4	1.12997	0
5	0.05381	134.4
6	0.04920	321.3
7	0.01509	129.2
8	0.01509	86.0
9	0.01114	297.9
10	0.15977	225.5
11	0.00863	332.6
12	0.13963	178.6
13	0.03210	321.3
14	0.00912	134.7
15	0.02651	321.0
16	0.09566	269.6
17	0.00744	83.8
18	0.03224	38.0
19	0.00848	215.4
20	0.02385	3.0
21	0.02582	149.7
22	0.05508	137.6
23	0.01538	191.0
24	0.03007	84.7
25	0.00690	354.6
26	0.01299	22.6
27	0.00385	81.4
28	0.00636	185.9
29	0.01460	311.9
30	0.02625	308.3

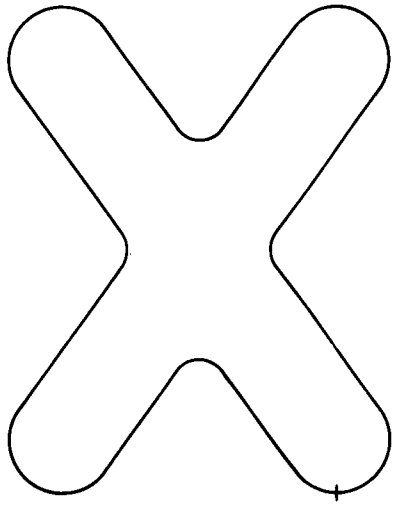

Fig. A-1

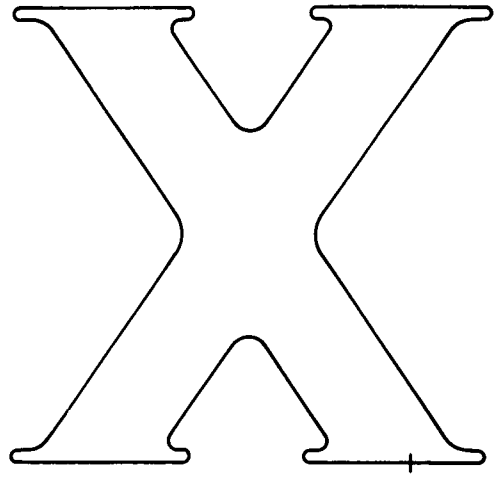

Fig. A-2

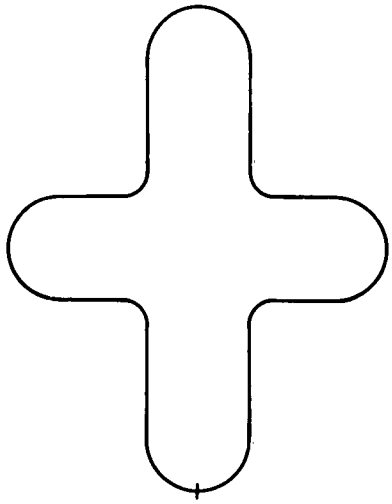

Fig. A-3

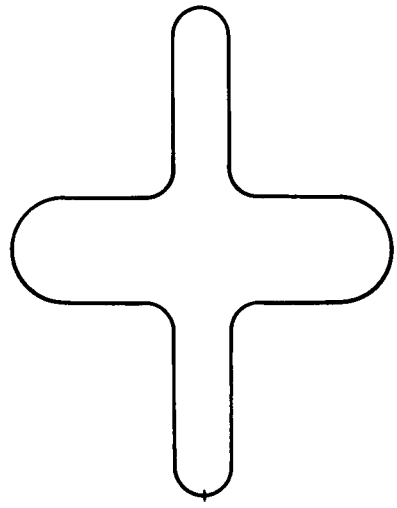

Fig. A-4

TABLE A-5

n	C_n (radians)	θ_n (degrees)
1	0.18132	237.6
2	0.50836	31.0
3	0.83554	0
4	0.08910	240.0
5	0.41821	118.3
6	0.45919	267.4
7	0.02783	356.7
8	0.12606	199.2
9	0.17844	358.2
10	0.00479	345.9
11	0.08830	114.7
12	0.02647	252.2
13	0.01775	13.1
14	0.08881	202.0
15	0.03439	356.7
16	0.00731	99.0
17	0.05563	303.4
18	0.05554	87.2
19	0.03037	36.3
20	0.02266	202.2
21	0.01334	41.6
22	0.03768	140.2
23	0.07218	292.9
24	0.02193	341.0
25	0.03225	4.1
26	0.03187	24.2
27	0.01256	200.9
28	0.02769	132.0
29	0.05099	270.3
30	0.02906	278.0

TABLE A-6

n	C_n (radians)	θ_n (degrees)
1	0.00386	279.0
2	0.92880	315.0
3	0.00590	287.4
4	1.11955	0
5	0.00421	248.8
6	0.17375	45.0
7	0.00514	251.1
8	0.13088	271.4
9	0.00373	279.8
10	0.00301	97.5
11	0.00452	270.4
12	0.03516	0
13	0.00463	268.6
14	0.03157	47.5
15	0.00511	228.4
16	0.02916	269.1
17	0.00548	252.9
18	0.01634	129.6
19	0.00175	57.7
20	0.03353	181.3
21	0.00673	157.2
22	0.01090	50.0
23	0.00533	241.0
24	0.00855	135.4
25	0.00389	28.6
26	0.00270	284.5
27	0.00349	155.1
28	0.01724	161.2
29	0.00674	322.7
30	0.00908	214.6

TABLE A-7

n	C_n (radians)	θ_n (degrees)
1	0.15678	17.7
2	0.76159	315.4
3	0.19806	250.4
4	1.12766	0
5	0.03730	285.0
6	0.10946	47.2
7	0.19057	335.4
8	0.00550	331.4
9	0.08302	27.4
10	0.08035	132.9
11	0.12021	72.8
12	0.07890	186.7
13	0.06498	113.9
14	0.03539	218.5
15	0.07926	165.8
16	0.07312	274.8
17	0.04877	195.4
18	0.02761	148.5
19	0.06082	250.8
20	0.02750	183.7
21	0.03293	294.6
22	0.00411	186.3
23	0.02704	338.5
24	0.00790	212.5
25	0.01456	24.0
26	0.00302	350.0
27	0.00160	98.9
28	0.00492	48.1
29	0.00415	63.9
30	0.01658	50.7

TABLE A-8

n	C_n (radians)	θ_n (degrees)
1	0.15578	180.0
2	0.20120	90.0
3	0.76483	0
4	0.02976	278.5
5	0.04008	2.4
6	0.29091	271.5
7	0.01744	171.3
8	0.01063	127.8
9	0.10926	186.2
10	0.01221	271.6
11	0.01691	5.7
12	0.03020	91.3
13	0.00503	200.7
14	0.02091	273.5
15	0.01577	150.0
16	0.01304	69.0
17	0.01349	189.3
18	0.02326	102.8
19	0.00530	50.7
20	0.00409	48.7
21	0.01042	356.9
22	0.00907	95.9
23	0.00283	219.1
24	0.00856	279.3
25	0.00530	289.8
26	0.01192	120.2
27	0.00580	330.0
28	0.01046	240.9
29	0.01741	0
30	0.01158	286.9

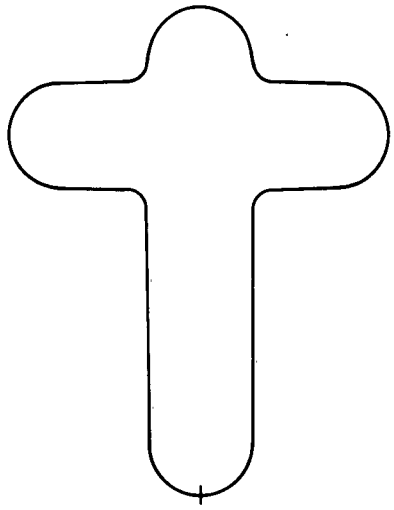

Fig. A-5

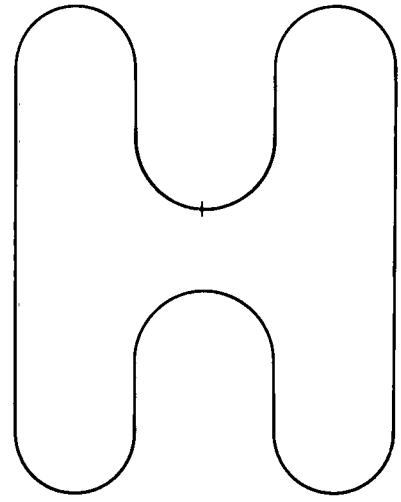

Fig. A-6

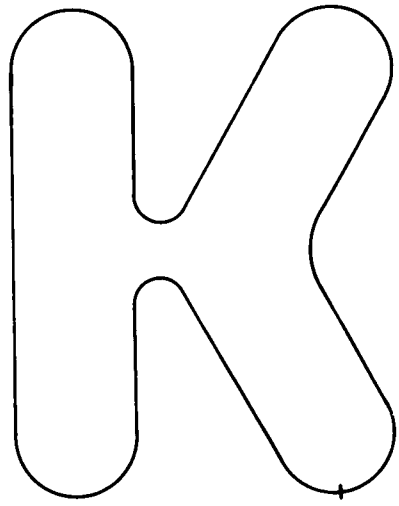

Fig. A-7

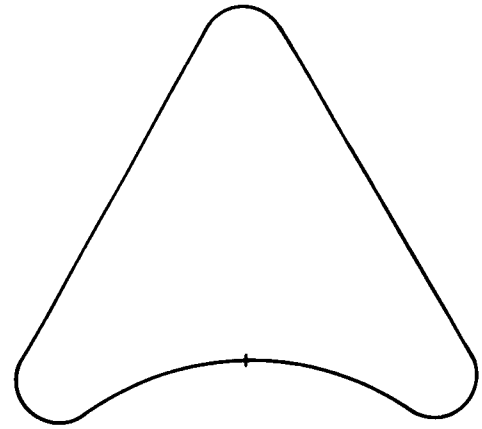

Fig. A-8

TABLE A-9

n	C_n (radians)	θ_n (degrees)
1	0.45017	331.5
2	0.73319	0
3	0.73124	95.7
4	0.24280	67.2
5	0.25604	21.5
6	0.13940	137.3
7	0.05386	105.0
8	0.09731	344.7
9	0.02687	285.0
10	0.04054	162.6
11	0.02501	165.0
12	0.02165	296.4
13	0.02973	194.9
14	0.03094	221.3
15	0.01085	38.5
16	0.01999	148.9
17	0.00716	247.5
18	0.00366	352.5
19	0.00553	158.7
20	0.01131	4.9
21	0.01467	344.8
22	0.00732	304.7
23	0.00232	104.7
24	0.00896	333.3
25	0.01025	288.2
26	0.00499	235.9
27	0.00027	51.6
28	0.00655	3.3
29	0.00332	87.4
30	0.00624	140.7

TABLE A-10

n	C_n (radians)	θ_n (degrees)
1	0.18701	180.0
2	0.30529	90.0
3	0.48218	0
4	0.17244	270.0
5	0.02245	185.0
6	0.19035	269.4
7	0.11342	178.0
8	0.06800	85.8
9	0.08453	176.0
10	0.06635	92.7
11	0.06394	353.0
12	0.02290	74.3
13	0.02845	6.8
14	0.03603	266.3
15	0.00768	310.0
16	0.01169	293.5
17	0.01217	175.5
18	0.00611	40.0
19	0.00256	13.1
20	0.00596	85.0
21	0.00178	280.3
22	0.01305	312.6
23	0.00314	307.0
24	0.01561	104.7
25	0.00891	190.0
26	0.00758	239.2
27	0.01784	323.1
28	0.00769	44.7
29	0.01104	109.1
30	0.01340	234.6

TABLE A-11

n	C_n (radians)	θ_n (degrees)
1	0.19264	174.0
2	0.27116	184.3
3	1.73745	0
4	0.29985	326.7
5	0.29780	155.7
6	0.22496	250.2
7	0.11154	198.5
8	0.21721	308.9
9	0.12889	190.0
10	0.20871	119.6
11	0.01312	210.0
12	0.18698	292.5
13	0.03749	297.3
14	0.14320	105.0
15	0.05475	139.5
16	0.08742	258.7
17	0.10340	260.6
18	0.06763	83.8
19	0.13367	66.6
20	0.01572	164.8
21	0.09953	215.9
22	0.06459	226.0
23	0.09865	1.8
24	0.09378	26.0
25	0.06272	160.3
26	0.07571	176.6
27	0.02559	114.4
28	0.07586	313.9
29	0.05388	315.0
30	0.05358	111.8

TABLE A-12

n	C_n (radians)	θ_n (degrees)
1	0.33029	202.6
2	0.48976	135.1
3	0.31800	67.5
4	0.52931	0
5	0.10239	295.0
6	0.13315	225.4
7	0.21108	157.5
8	0.11986	92.5
9	0.11189	202.0
10	0.07774	314.7
11	0.07655	248.0
12	0.06278	178.2
13	0.06747	116.5
14	0.04891	53.1
15	0.03417	344.5
16	0.05841	270.0
17	0.03576	193.7
18	0.02695	111.0
19	0.02017	39.0
20	0.00859	350.5
21	0.01615	316.4
22	0.01778	269.2
23	0.01449	183.8
24	0.00890	87.6
25	0.00901	343.0
26	0.00617	154.7
27	0.00411	62.3
28	0.00067	95.7
29	0.00235	188.8
30	0.00327	78.3

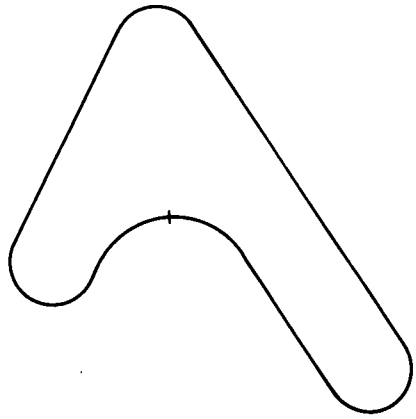

Fig. A-9

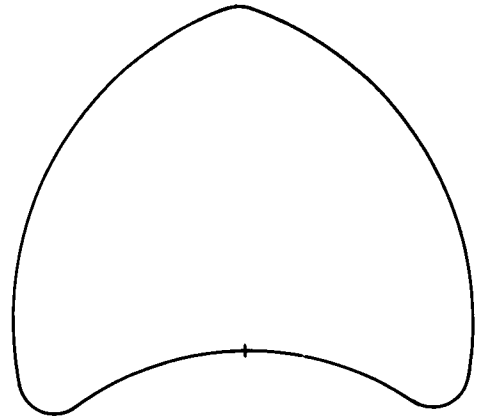

Fig. A-10

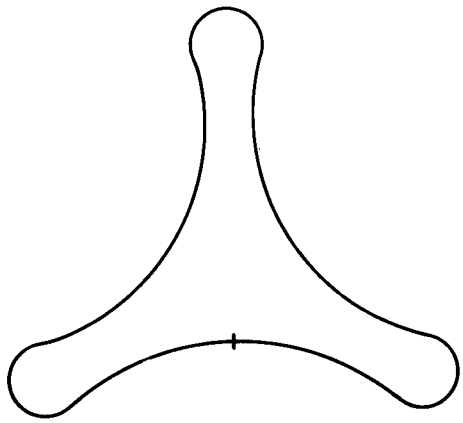

Fig. A-11

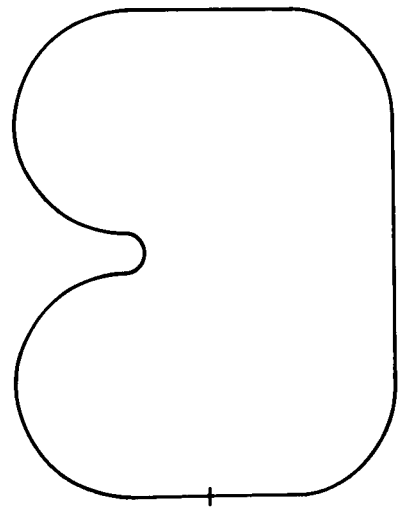

Fig. A-12

TABLE A-13

n	C_n (radians)	θ_n (degrees)
1	0.67406	315.0
2	1.05550	0
3	0.11611	47.0
4	0.39255	92.0
5	1.01577	316.0
6	0.29829	0
7	0.33987	46.5
8	0.12395	87.8
9	0.04081	130.5
10	0.25529	181.4
11	0.20659	225.9
12	0.02840	84.9
13	0.03299	310.0
14	0.21372	181.8
15	0.00824	28.4
16	0.06362	270.7
17	0.00732	330.8
18	0.01529	354.1
19	0.00773	232.8
20	0.01660	277.6
21	0.07976	317.9
22	0.02958	355.6
23	0.08719	45.0
24	0.03645	98.6
25	0.06179	236.7
26	0.00702	172.8
27	0.00879	187.6
28	0.04002	98.8
29	0.00518	124.5
30	0.02767	182.4

TABLE A-14

n	C_n (radians)	θ_n (degrees)
1	0.00417	336.7
2	1.25527	0
3	0.00789	123.5
4	1.11647	77.7
5	0.00996	290.1
6	0.24855	49.0
7	0.00860	96.9
8	0.13876	152.3
9	0.01138	265.0
10	0.32207	333.6
11	0.00872	44.2
12	0.12209	9.4
13	0.00590	190.5
14	0.15725	42.9
15	0.00158	259.1
16	0.10050	185.9
17	0.00201	234.2
18	0.04944	266.2
19	0.00080	44.5
20	0.06979	305.2
21	0.00149	129.2
22	0.02016	43.7
23	0.00282	114.5
24	0.05217	99.7
25	0.00350	207.7
26	0.03628	172.4
27	0.00299	1.1
28	0.02655	276.1
29	0.00265	116.9
30	0.04381	342.8

TABLE A-15

n	C_n (radians)	θ_n (degrees)
1	0.01112	320.5
2	1.68324	0
3	0.00246	338.3
4	0.88153	110.6
5	0.00376	18.5
6	0.31594	295.8
7	0.00460	312.4
8	0.07062	206.9
9	0.00711	48.0
10	0.20313	37.2
11	0.01141	192.6
12	0.17708	172.2
13	0.00715	327.3
14	0.05627	346.1
15	0.00279	258.3
16	0.02473	261.5
17	0.00983	305.2
18	0.02961	87.5
19	0.00435	353.8
20	0.01398	193.4
21	0.01028	82.4
22	0.00716	118.8
23	0.01036	206.8
24	0.01568	228.1
25	0.00761	319.9
26	0.02601	333.9
27	0.00603	36.0
28	0.01559	100.7
29	0.01392	115.4
30	0.01017	145.5

TABLE A-16

n	C_n (radians)	θ_n (degrees)
1	0.62124	321.2
2	0.90362	0
3	0.56880	63.4
4	0.33831	325.7
5	0.11394	348.0
6	0.16128	159.3
7	0.13561	266.9
8	0.10559	224.7
9	0.06170	200.1
10	0.06421	323.5
11	0.04329	295.0
12	0.03679	48.4
13	0.02078	49.0
14	0.01568	226.0
15	0.04352	135.5
16	0.03389	181.8
17	0.01661	212.9
18	0.01495	169.0
19	0.1001	298.1
20	0.1186	8.4
21	0.01256	346.6
22	0.00887	35.2
23	0.01027	119.8
24	0.00514	9.3
25	0.01436	149.4
26	0.01070	156.1
27	0.00749	8.9
28	0.00808	203.8
29	0.00537	61.0
30	0.00908	11.4

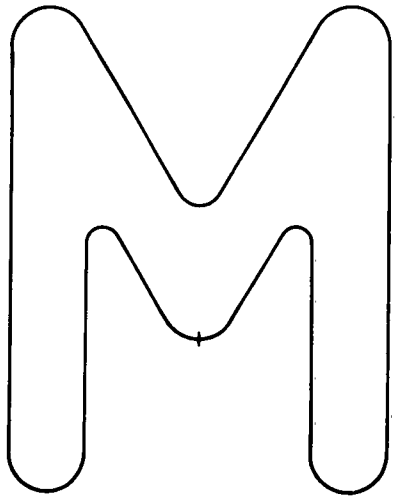

Fig. A-13

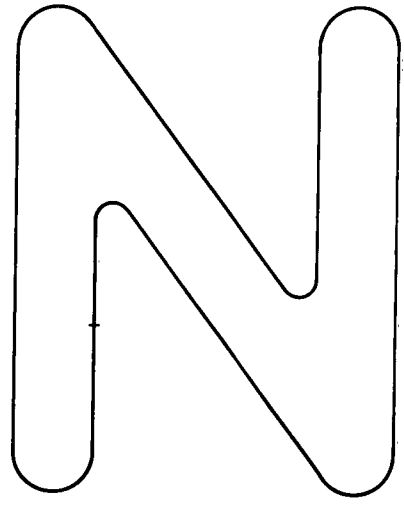

Fig. A-14

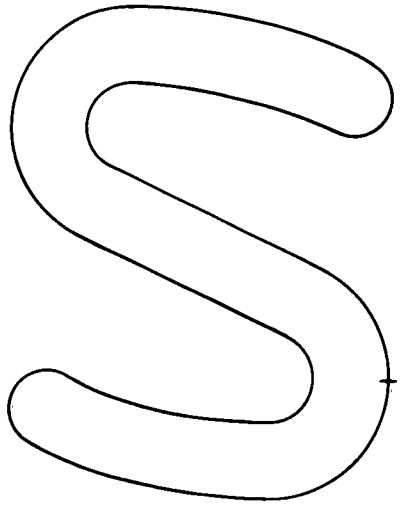

Fig. A-15

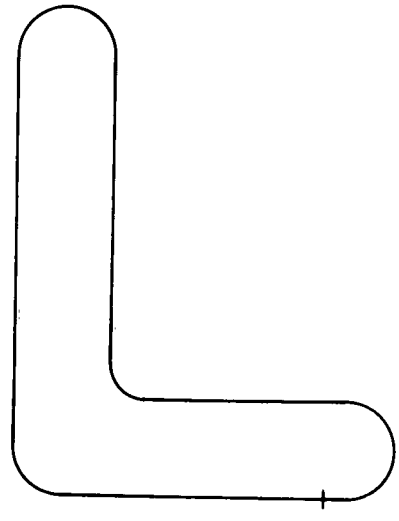

Fig. A-16

TABLE A-17

n	C_n (radians)	θ_n (degrees)
1	1.37346	0
2	1.01837	90.0
3	0.71524	179.9
4	0.01594	91.0
5	0.37941	179.7
6	0.20202	90.0
7	0.05907	179.8
8	0.10910	269.5
9	0.18171	180.2
10	0.14010	269.5
11	0.00465	352.8
12	0.08159	89.6
13	0.00814	184.9
14	0.11935	270.7
15	0.03050	358.6
16	0.05180	89.0
17	0.04661	178.6
18	0.00509	79.4
19	0.01953	7.3
20	0.02125	269.6
21	0.02484	178.6
22	0.01242	97.9
23	0.02688	177.5
24	0.02718	263.7
25	0.02376	357.9
26	0.00348	109.8
27	0.02615	187.3
28	0.01830	269.7
29	0.01873	352.8
30	0.00550	80.9

TABLE A-18

n	C_n (radians)	θ_n (degrees)
1	0.80343	60.3
2	0.69239	209.3
3	1.04981	0
4	0.00626	51.1
5	0.01313	270.0
6	0.10396	272.1
7	0.25286	241.6
8	0.13187	32.7
9	0.13989	181.7
10	0.00927	321.4
11	0.07212	119.7
12	0.03951	270.4
13	0.04896	60.8
14	0.03222	216.0
15	0.05318	0
16	0.05950	152.9
17	0.03137	292.9
18	0.02098	99.6
19	0.00763	231.9
20	0.03360	40.7
21	0.02134	166.5
22	0.03254	333.7
23	0.01543	108.6
24	0.02626	284.3
25	0.00358	28.0
26	0.00889	218.6
27	0.00459	335.3
28	0.02471	158.7
29	0.01607	303.0
30	0.01224	83.3

TABLE A-19

n	C_n (radians)	θ_n (degrees)
1	0.71143	132.8
2	1.28320	0
3	0.35277	299.4
4	0.23462	97.1
5	0.60846	150.5
6	0.45176	332.9
7	0.19635	280.9
8	0.07294	30.2
9	0.24822	119.4
10	0.07517	348.5
11	0.07939	251.7
12	0.01794	183.0
13	0.02049	297.0
14	0.04298	42.5
15	0.01564	357.6
16	0.05194	112.4
17	0.02238	221.9
18	0.00920	238.1
19	0.02239	321.9
20	0.01423	235.3
21	0.04498	53.2
22	0.01088	152.6
23	0.01531	82.0
24	0.05326	213.0
25	0.03198	5.6
26	0.00912	293.5
27	0.02105	53.7
28	0.02094	157.0
29	0.00166	241.4
30	0.01169	203.9

TABLE A-20

n	C_n (radians)	θ_n (degrees)
1	0.73789	317.0
2	0.47380	325.9
3	0.92259	0
4	0.61656	47.8
5	0.25036	271.0
6	0.16130	5.8
7	0.07691	57.0
8	0.07367	208.2
9	0.16536	162.8
10	0.11187	225.2
11	0.01615	41.8
12	0.09021	8.6
13	0.04863	305.2
14	0.01081	37.3
15	0.04687	263.0
16	0.04428	344.1
17	0.02516	154.7
18	0.01940	282.7
19	0.01377	136.0
20	0.01678	222.6
21	0.03366	42.6
22	0.01867	141.1
23	0.01814	338.7
24	0.02529	66.5
25	0.01069	38.4
26	0.01194	126.9
27	0.01149	121.1
28	0.01793	201.2
29	0.00595	151.3
30	0.02005	182.5

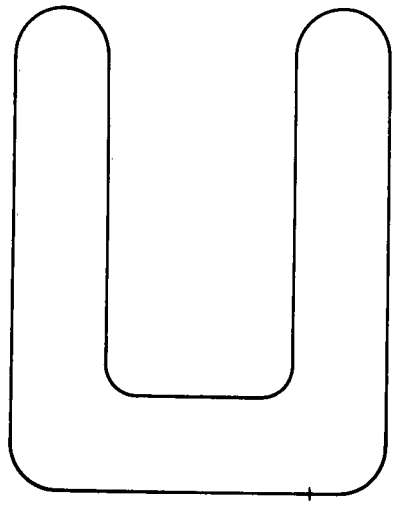

Fig. A-17

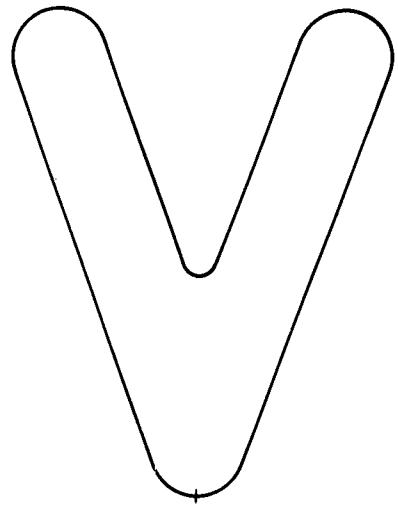

Fig. A-18

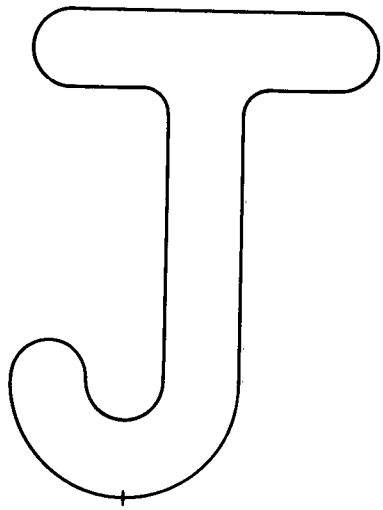

Fig. A-19

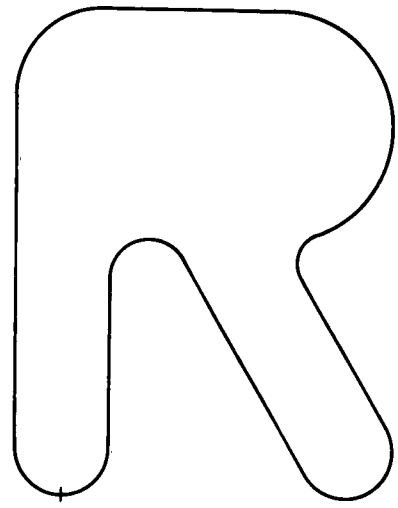

Fig. A-20

TABLE A-21

n	C_n (radians)	θ_n (degrees)
1	0.94561	0
2	0.73773	101.3
3	0.51114	260.9
4	0.83353	350.3
5	0.30673	353.6
6	0.30429	50.5
7	0.03186	232.7
8	0.05296	320.4
9	0.10024	179.5
10	0.03338	329.8
11	0.05563	156.1
12	0.05274	177.4
13	0.01885	241.8
14	0.01779	95.4
15	0.03886	200.0
16	0.04954	260.5
17	0.04045	315.9
18	0.01766	116.9
19	0.06719	238.4
20	0.04540	312.9
21	0.02744	15.7
22	0.02506	100.0
23	0.01978	191.3
24	0.01054	26.0
25	0.01454	131.6
26	0.00672	188.3
27	0.00699	231.3
28	0.00424	88.9
29	0.00250	74.8
30	0.00502	159.0

TABLE A-21a

n	C_n (radians)	θ_n (degrees)
1	1.02028	0
2	0.65224	101.8
3	0.57255	283.2
4	0.93868	2.1
5	0.23304	15.7
6	0.25303	80.7
7	0.11183	231.4
8	0.03315	271.4
9	0.11909	193.7
10	0.02981	38.8
11	0.07432	166.6
12	0.03313	167.4
13	0.02875	73.7
14	0.05384	114.4
15	0.02709	171.3
16	0.02478	87.5
17	0.06896	116.4
18	0.09441	157.3
19	0.04588	188.6
20	0.09236	131.8
21	0.11687	164.0
22	0.10933	187.4
23	0.07711	204.3
24	0.06881	189.0
25	0.08401	211.9
26	0.06458	223.5
27	0.06432	225.7
28	0.06361	228.8
29	0.06228	246.0
30	0.06012	254.5

TABLE A-21ab

n	C_n (radians)	θ_n (degrees)
1	1.14718	0
2	0.73425	106.3
3	0.56927	282.7
4	0.87324	5.5
5	0.36912	13.5
6	0.26244	104.8
7	0.08265	302.3
8	0.08133	169.9
9	0.15951	254.9
10	0.11883	91.0
11	0.12442	215.4
12	0.03362	26.5
13	0.09730	144.1
14	0.04228	282.6
15	0.09688	94.5
16	0.09842	208.9
17	0.07273	28.7
18	0.16206	150.0
19	0.11330	237.9
20	0.05070	95.0
21	0.16520	174.0
22	0.10434	235.7
23	0.07804	185.3
24	0.12659	236.5
25	0.02920	273.0
26	0.09671	220.0
27	0.09604	278.4
28	0.02591	266.2
29	0.08475	250.9
30	0.07931	307.2

TABLE A-21abc

n	C_n (radians)	θ_n (degrees)
1	0.07259	0
2	0.74687	81.1
3	0.46984	240.4
4	0.82289	348.5
5	0.53372	7.5
6	0.15405	54.2
7	0.20872	111.5
8	0.21857	308.2
9	0.30073	166.1
10	0.23018	329.8
11	0.21025	165.6
12	0.07969	72.4
13	0.14668	274.6
14	0.23974	120.0
15	0.14295	311.2
16	0.09314	309.0
17	0.07193	118.2
18	0.08033	280.0
19	0.14486	91.0
20	0.15574	177.0
21	0.04829	311.2
22	0.10947	133.9
23	0.14418	148.8
24	0.10187	243.5
25	0.15029	148.7
26	0.08887	246.4
27	0.07060	202.6
28	0.06696	158.4
29	0.12700	249.3
30	0.03376	181.4

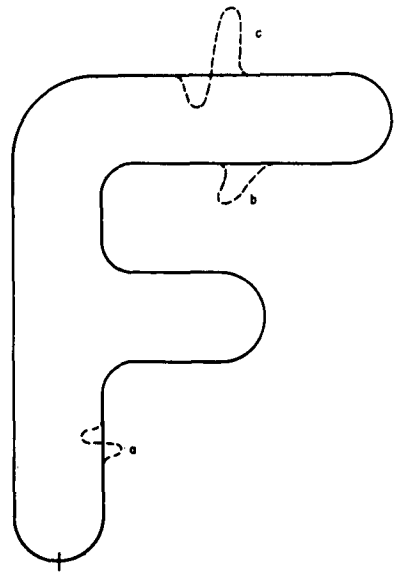

Figure A-21 is used for the specific purpose of determining whether small random distortions can be added to a smooth character such that recognition is still possible. From this point, Fig. A-21 will signify the smooth character with no distortions. Fig. A-21a is the same as Fig. A-21 except for distortion a. Fig. A-21ab is the same as Fig. A-21a except for distortion b. Fig. A-21abc is the same Fig. A-21ab except for distortion c. The tables and all further references to the above character will have this same designation.

TABLE A-22

n	C_n (radians)	θ_n (degrees)
1	1.40530	0
2	0.64045	90.0
3	0.46832	0
4	0.84175	89.9
5	0.71521	180.0
6	0.04711	88.4
7	0.20639	0
8	0.23300	89.1
9	0.00443	173.7
10	0.04713	89.8
11	0.05917	179.5
12	0.11036	90.0
13	0.03681	180.5
14	0.03680	89.4
15	0.02240	182.6
16	0.04125	274.6
17	0.02582	0
18	0.00632	119.4
19	0.02615	354.7
20	0.04146	88.7
21	0.05282	178.3
22	0.04282	276.0
23	0.01249	0
24	0.04440	266.7
25	0.06117	356.2
26	0.03521	85.7
27	0.03513	176.0
28	0.02511	285.0
29	0.00776	53.8
30	0.01841	259.3

TABLE A-23

n	C_n (radians)	θ_n (degrees)
1	1.69383	0
2	1.16851	90.2
3	0.07265	177.6
4	0.43258	92.0
5	0.40096	181.9
6	0.02313	90.6
7	0.23669	182.5
8	0.07667	276.5
9	0.11679	179.7
10	0.11986	268.1
11	0.02577	206.4
12	0.09164	280.5
13	0.02004	27.1
14	0.04579	256.2
15	0.03383	351.9
16	0.01614	293.3
17	0.03288	9.6
18	0.01207	80.2
19	0.00141	46.4
20	0.00661	260.3
21	0.01469	305.1
22	0.01132	86.9
23	0.01375	159.9
24	0.01346	253.1
25	0.00695	317.7
26	0.01108	273.9
27	0.00304	36.6
28	0.00984	5.9
29	0.00903	16.6
30	0.01619	203.2

TABLE A-24

n	C_n (radians)	θ_n (degrees)
1	2.26839	0
2	1.37000	76.4
3	0.13422	111.9
4	0.48964	87.5
5	0.42688	167.4
6	0.15578	345.6
7	0.28373	221.9
8	0.16390	233.9
9	0.20547	252.6
10	0.25040	319.3
11	0.26029	29.2
12	0.06912	349.7
13	0.17473	49.0
14	0.12521	131.6
15	0.08736	311.4
16	0.05626	59.2
17	0.04366	286.5
18	0.01570	287.7
19	0.07321	300.7
20	0.07640	11.2
21	0.02191	65.4
22	0.03286	33.2
23	0.05914	156.8
24	0.08460	238.7
25	0.04971	322.2
26	0.01265	144.7
27	0.02864	275.5
28	0.00707	56.6
29	0.02210	255.5
30	0.00377	263.9

TABLE A-25

n	C_n (radians)	θ_n (degrees)
1	0.92597	0
2	0.89842	76.7
3	0.77441	4.7
4	0.10538	325.4
5	0.04981	62.8
6	0.20652	357.6
7	0.17441	288.6
8	0.05324	205.5
9	0.02939	73.7
10	0.03963	310.7
11	0.03463	178.7
12	0.05541	61.1
13	0.04692	358.0
14	0.03786	291.7
15	0.00959	203.4
16	0.01526	336.4
17	0.01725	285.9
18	0.01791	241.2
19	0.00396	173.9
20	0.00551	128.3
21	0.01353	62.0
22	0.00263	357.2
23	0.01286	294.0
24	0.01552	298.6
25	0.01240	344.3
26	0.00830	200.5
27	0.01126	177.1
28	0.00409	136.5
29	0.01083	308.2
30	0.00528	205.2

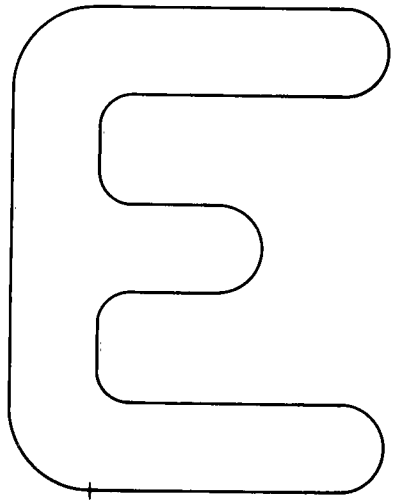

Fig. A-22

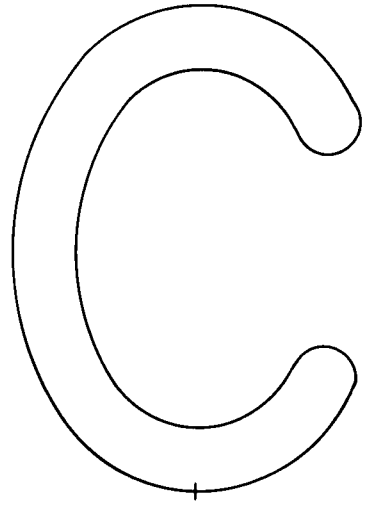

Fig. A-23

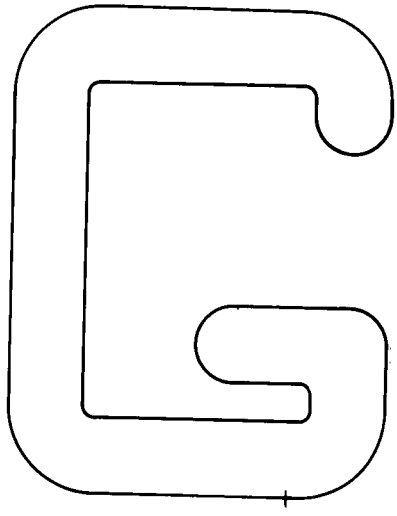

Fig. A-24

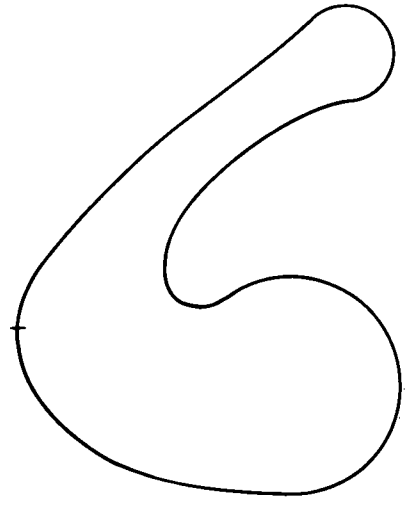

Fig. A-25

TABLE A-26

n	C_n (radians)	θ_n (degrees)
1	1.49255	0
2	0.73741	21.6
3	0.74700	129.7
4	0.51512	319.2
5	0.08617	17.7
6	0.25424	21.7
7	0.35310	320.3
8	0.31343	232.3
9	0.37780	223.7
10	0.39239	33.0
11	0.25371	213.2
12	0.26004	187.9
13	0.34393	239.8
14	0.14790	136.0
15	0.17156	48.0
16	0.27042	300.4
17	0.15444	13.8
18	0.09539	85.2
19	0.30929	255.3
20	0.01090	208.1
21	0.27003	190.3
22	0.20117	33.2
23	0.15339	0
24	0.15300	337.1
25	0.07412	142.6
26	0.17418	177.9
27	0.09343	149.7
28	0.20590	20.5
29	0.25262	197.1
30	0.07412	214.8

TABLE A-27

n	C_n (radians)	θ_n (degrees)
1	0.18294	344.0
2	0.50776	0
3	0.27721	63.0
4	0.18046	103.1
5	0.49176	101.1
6	0.22467	85.8
7	0.12724	146.6
8	0.17333	94.6
9	0.17042	334.7
10	0.15018	312.2
11	0.14000	272.2
12	0.11519	20.1
13	0.14169	167.4
14	0.30230	90.9
15	0.18094	106.6
16	0.27396	120.4
17	0.16883	101.6
18	0.12715	165.6
19	0.07707	223.5
20	0.25881	216.2
21	0.13745	236.7
22	0.20133	218.4
23	0.07485	258.0
24	0.06060	233.4
25	0.01277	335.9
26	0.07993	5.2
27	0.03996	307.5
28	0.06483	356.5
29	0.09457	254.4
30	0.04685	225.9

TABLE A-28

n	C_n (radians)	θ_n (degrees)
1	0.28141	0
2	0.03533	106.8
3	0.21043	228.3
4	0.15079	329.4
5	0.10172	172.0
6	0.14767	213.8
7	0.00980	301.6
8	0.21831	167.8
9	0.11033	262.7
10	0.12366	258.9
11	0.18003	316.8
12	0.13288	326.4
13	0.11299	349.3
14	0.09708	340.4
15	0.08048	109.4
16	0.18493	219.2
17	0.19441	282.5
18	0.23299	347.9
19	0.28324	74.1
20	0.24924	134.7
21	0.22532	206.8
22	0.21038	305.9
23	0.11212	3.0
24	0.10116	99.5
25	0.12268	204.9
26	0.08684	219.2
27	0.10238	268.8
28	0.12847	256.6
29	0.12894	303.3
30	0.10288	354.8

TABLE A-29

n	C_n (radians)	θ_n (degrees)
1	0.69808	140.9
2	0.55930	51.0
3	1.07991	0
4	0.48538	262.3
5	0.62145	347.0
6	0.33318	183.8
7	0.35756	183.7
8	0.67655	134.5
9	0.21464	161.0
10	0.24987	24.3
11	0.38621	19.5
12	0.24791	280.6
13	0.21620	266.5
14	0.09143	226.8
15	0.07579	278.3
16	0.15160	105.4
17	0.08330	102.2
18	0.02872	313.4
19	0.13930	68.6
20	0.14571	142.3
21	0.06730	0
22	0.10220	315.0
23	0.13353	300.4
24	0.05875	271.0
25	0.11746	157.2
26	0.12062	165.6
27	0.13151	92.2
28	0.10625	123.6
29	0.05300	292.3
30	0.18032	333.0

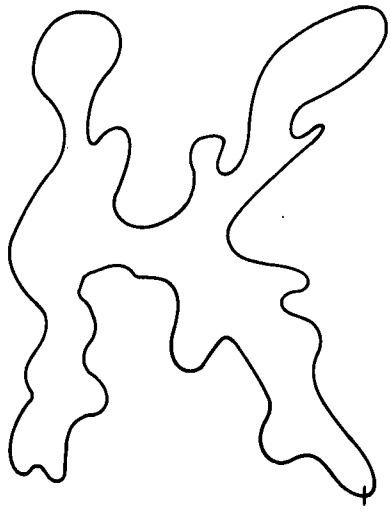

Fig. A-26

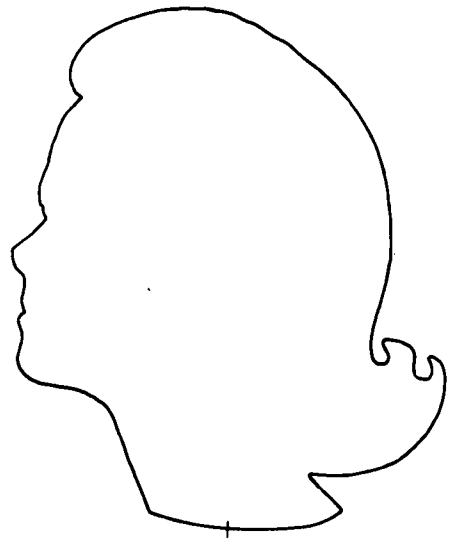

Fig. A-27

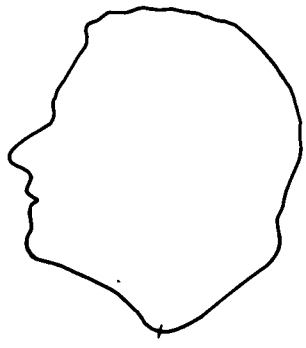

Fig. A-28

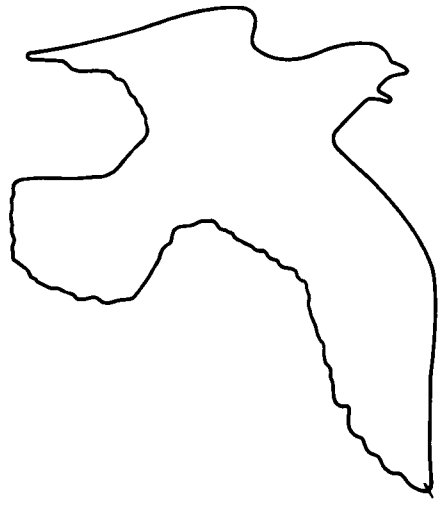

Fig. A-29

TABLE A-30

n	C_n (radians)	θ_n (degrees)
1	0.24713	186.3
2	0.60886	212.8
3	0.69494	0
4	0.15880	36.0
5	0.62252	191.0
6	0.49496	18.7
7	0.26073	125.5
8	0.66488	11.2
9	0.75150	27.3
10	0.50462	61.8
11	0.22427	55.0
12	0.58613	195.1
13	0.35253	18.9
14	0.51894	134.6
15	0.44721	0
16	0.16570	175.7
17	0.17320	68.8
18	0.33780	262.4
19	0.16540	45.4
20	0.20032	309.2
21	0.14720	205.9
22	0.27010	60.5
23	0.09187	258.5
24	0.10759	22.3
25	0.14523	316.9
26	0.12966	162.4
27	0.32582	0
28	0.37775	254.8
29	0.32237	45.7
30	0.36782	224.2

TABLE A-31

n	C_n (radians)	θ_n (degrees)
1	0.71937	262.0
2	0.20640	226.0
3	0.44490	334.6
4	0.33284	140.7
5	0.69082	0
6	0.94533	0
7	0.40679	333.2
8	0.15197	72.0
9	0.35363	183.0
10	0.25597	244.3
11	0.21751	1.9
12	0.20628	327.0
13	0.35741	182.5
14	0.22453	318.8
15	0.04566	12.8
16	0.06600	71.6
17	0.28274	142.2
18	0.18806	240.9
19	0.30820	115.6
20	0.25422	5.5
21	0.08733	130.2
22	0.10982	322.5
23	0.04226	92.9
24	0.04540	20.0
25	0.06272	97.3
26	0.02464	169.5
27	0.11903	196.2
28	0.04500	142.5
29	0.10256	277.3
30	0.03768	78.0

TABLE A-32

n	C_n (radians)	θ_n (degrees)
1	1.03383	342.8
2	0.61643	320.9
3	1.10194	0
4	0.26106	61.5
5	0.58477	331.1
6	0.24013	310.5
7	0.69522	192.7
8	0.31971	241.2
9	0.49659	178.5
10	0.13865	319.5
11	0.12325	314.7
12	0.25928	265.1
13	0.24825	228.0
14	0.13614	201.0
15	0.76324	193.6
16	0.42353	304.0
17	0.05938	320.0
18	0.28227	211.9
19	0.08534	152.0
20	0.27928	138.5
21	0.05289	336.2
22	0.10778	258.4
23	0.07581	55.0
24	0.12992	74.2
25	0.22784	90.0
26	0.01655	142.7
27	0.07438	250.0
28	0.22458	336.4
29	0.06235	19.5
30	0.03872	298.0

TABLE A-33

n	C_n (radians)	θ_n (degrees)
1	0.70910	0
2	0.27655	257.9
3	0.62390	174.4
4	0.35956	326.2
5	0.15971	347.2
6	0.28762	30.5
7	0.38245	354.3
8	0.42431	130.1
9	0.58665	44.5
10	0.77958	300.1
11	0.34361	193.5
12	0.73230	346.7
13	0.84925	248.5
14	0.41102	130.8
15	0.15476	43.0
16	0.29459	211.1
17	0.08567	162.5
18	0.25862	227.2
19	0.36321	131.6
20	0.36581	35.2
21	0.50341	225.8
22	0.01018	105.5
23	0.98621	17.2
24	0.51067	255.3
25	0.30495	44.7
26	0.33738	244.5
27	0.08243	2.4
28	0.21857	349.6
29	0.25613	248.7
30	0.27364	136.6

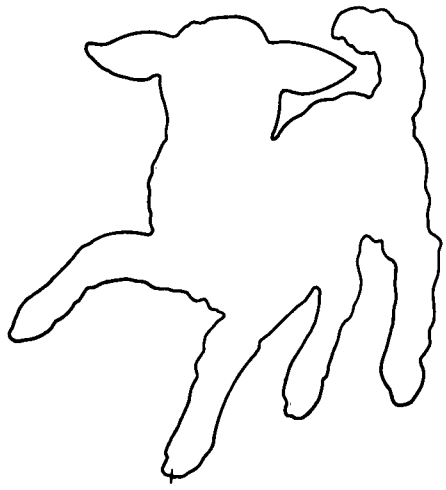

Fig. A-30

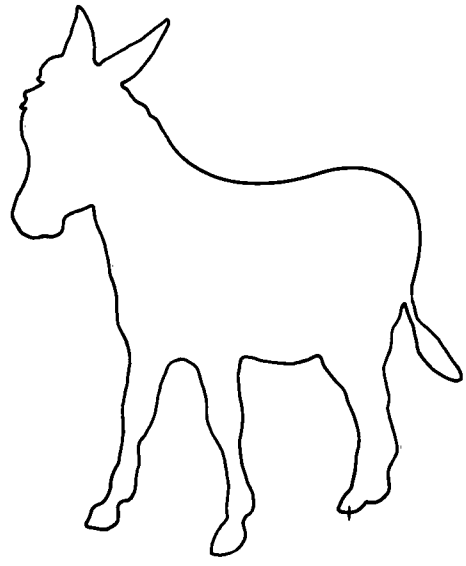

Fig. A-31

Fig. A-32

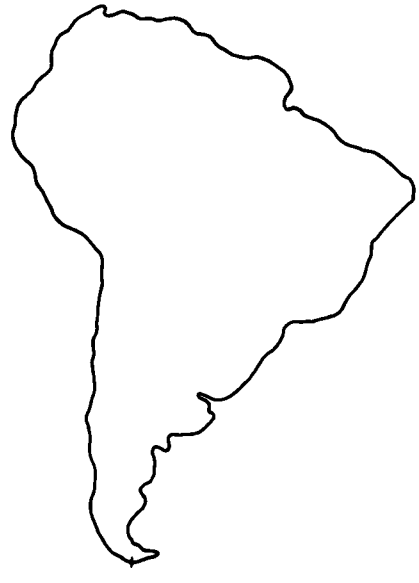

Fig. A-33

TABLE A-34

n	C_n (radians)	θ_n (degrees)
1	0.12045	225.2
2	0.17443	43.4
3	0.36744	0
4	0.26564	318.8
5	0.13335	288.7
6	0.13581	263.3
7	0.09354	244.3
8	0.09229	191.5
9	0.08173	150.5
10	0.05016	265.8
11	0.08323	109.8
12	0.05591	70.0
13	0.05458	63.0
14	0.05035	11.61
15	0.03143	344.0
16	0.03838	327.0
17	0.04250	263.2
18	0.03700	234.3
19	0.02620	214.9
20	0.02831	170.3
21	0.01786	134.9
22	0.02540	150.9
23	0.03971	85.1
24	0.01375	4.0
25	0.01140	32.9
26	0.03540	7.7
27	0.01624	311.4
28	0.02126	240.5
29	0.02357	241.3
30	0.02378	280.5

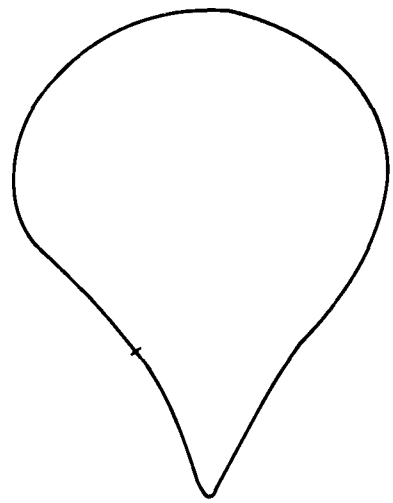

Fig. A-34

APPENDIX II

TESTING OF DIGITAL COMPUTER RESULTS

The testing of digital computer programming and results was accomplished by using the character in Fig. 2-1. This character has a defining function G (ℓ_1) for which the Fou. ier series is readily calculated. Table A-35 gives the computer and calculated results for the test character. The error in the calculation of coefficients exceeds 20 per cent for terms greater than the sixteenth harmonic. However, only 240 points were used to define the character in the x-y plane. These points were not uniformly spaced. The computation of the thirtieth harmonic coefficient results in a point on the defining curve every $\pi/4$ radians on the average. All subsequent characters have been represented by a minimum of 450 points and in most cases 550 or more points were used. Also, these points were more uniformly spaced than for the test character.

Two of the representative series calculated by the digital computer have been plotted using only the dominant terms. An analogue computer was used for this task. Seven terms from the series in Table A-3 are shown graphically in Fig. A-36. The calculated results are shown in Fig. A-35. Twenty one terms from the series in Table A-2 are shown as Fig. A-38. Fig. A-37 is the calculated result for this case.

These checks on digital computer performance indicate that acceptable accuracy is obtained in the calculations.

TABLE A-35

FOURIER COSINE SERIES COEFFICIENTS

AND PHASE ANGLES FOR FIGURE 2-1a

	Computer Results		Calculated Results	
n	C_n (radians)	ϕ_n (degrees)	C_n (radians)	ϕ_n (degrees)
1	0.00040	213.7	0	-
2	0.00035	-84.6	0	-
3	0.00319	85.6	0	-
4	0.48787	90.0	0.50000	90°
5	0.00069	-50.4	0	-
6	0.00925	267.7	0	-
7	0.00343	-69.7	0	-
8	0.24692	-89.8	0.25000	-90°
9	0.00440	96.5	0	-
10	0.00252	83.9	0	-
11	0.00527	113.5	0	-
12	0.14633	89.4	0.16666	90°
13	0.00312	81.2	0	-
14	0.01255	-87.2	0	-
15	0.00178	216.6	0	-
16	0.10451	-88.6	0.12500	-90°
17	0.00383	48.8	0	-
18	0.00579	226.9	0	-
19	0.00374	-54.9	0	-
20	0.06163	94.3	0.10000	90°
21	0.00814	97.4	0	-
22	0.00512	-89.7	0	-
23	0.00654	262.1	0	-
24	0.05158	-97.3	0.08333	-90°
25	0.00275	-10.2	0	-
26	0.01760	-73.3	0	-
27	0.00408	102.2	0	-
28	0.03036	89.8	0.07142	90°
29	0.00292	78.0	0	-
30	0.01345	81.7	0	-

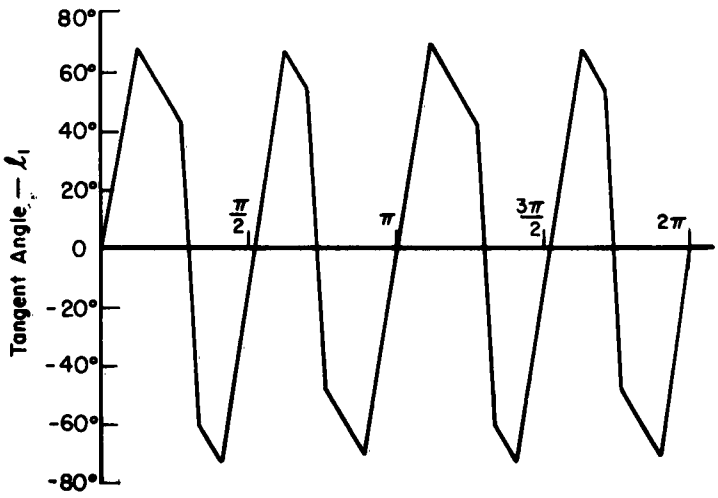

Fig. A-35

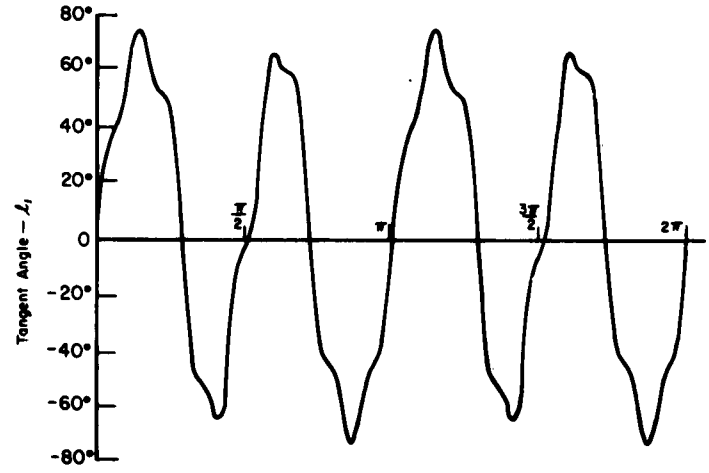

Fig. A-36

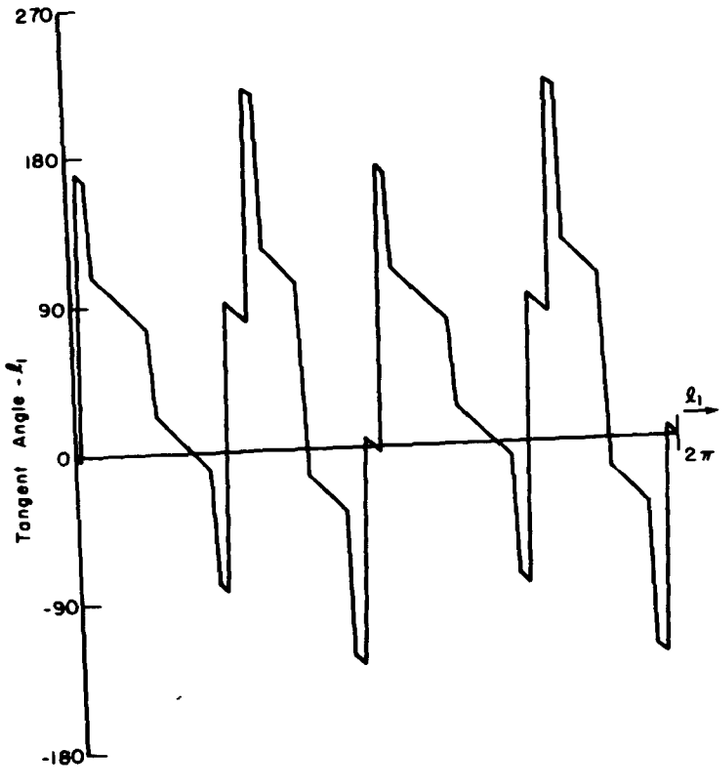

Fig. A-37

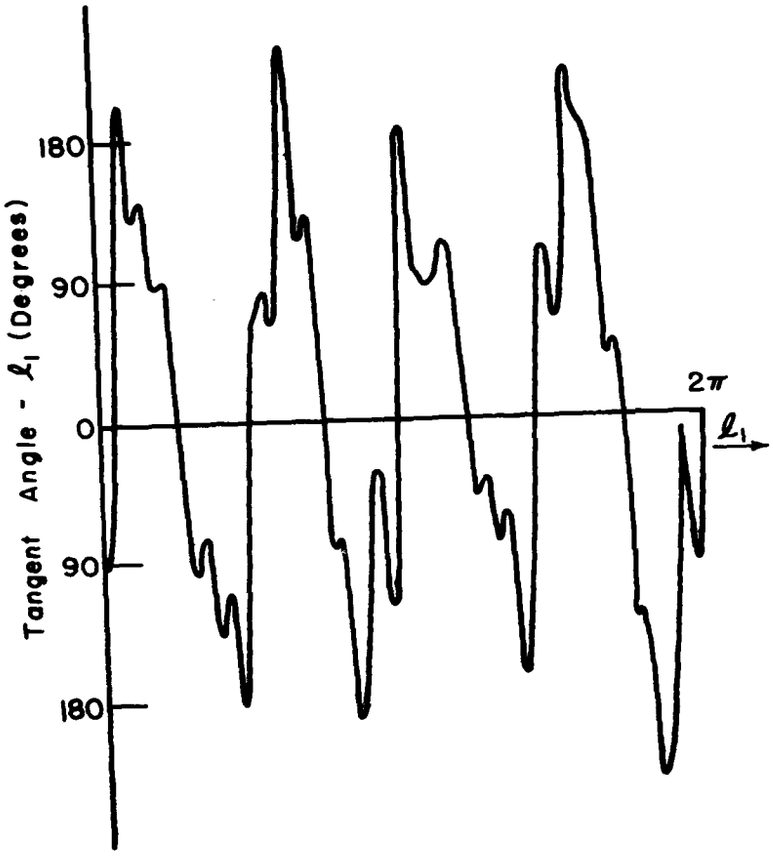

Fig. A-38

BIBLIOGRAPHY

1. Greanias, E.C., "Design of Logic for Recognition of Printed Characters by Simulation", IBM Journal, Vol. 1, January 1957, pp. 8-18.

2. Dimond, T.L., "Devices for Reading Handwritten Characters", Proceedings of EJCC , 1957, pp. 232-237 .

3. Gill, A., "Minimum Scan Pattern Recognition", IRE Transactions on Information Theory, June 1959.

4. Unger, S.H., "Pattern Detection and Recognition", IRE Proceedings, October 1959, pp. 1737-1752.

5. Cosgriff, R.L., "Identification of Shape", Report 820-11, 15 Dec. 1960, Antenna Laboratory, The Ohio State University Research Foundation; prepared under Contract AF 33(616)-5590 with Aeronautical Systems Division, Air Force Systems Command, United States Air Force, Wright-Patterson Air Force Base, Ohio.

PROJECT 1222
REPORT DISTRIBUTION LIST
Contract AF 33(616)-7843

Copies	
3	Commander Aeronautical Systems Division Attn: WCLGGEG Wright-Patterson Air Force Base, Ohio
1	Commander Aeronautical Systems Division Attn: WWAD Wright-Patterson Air Force Base, Ohio
1	Commander Aeronautical Systems Division Attn: WWAT Wright-Patterson Air Force Base, Ohio
1	Commander Air Research and Development Command Attn: RDRD Andrews Air Force Base Washington 25, D.C.
1	Commander Air Research and Development Command Attn: RDRC Andrews Air Force Base Washington 25, D.C.
1	Director Air University Attn: 7575, Library Maxwell Air Force Base, Alabama
1	Director of Research and Technology Headquarters, USAF Attn: AFDRT-ER Washington 25, D.C.
1	Director Naval Research Laboratories Attn: Code 2021 Washington 25, D.C.

Copies

1 Commander
Air Force Cambridge Research Center
Attn: Electronics Research Library
L.G. Hanscom Field
Bedford, Massachusetts

1 Commander
Rome Air Development Center
Attn: Research Library RCRES-4C
Griffiss Air Force Base, New York

1 The Franklin Institute Laboratories
Attn: A.C. Byer
Benjamin Franklin Parkway and 20th Streets
Philadelphia, Pennsylvania

1 Goodyear Aircraft Corporation
1210 Massillon Road
Akron 15, Ohio

1 Johns Hopkins University
Applied Physics Laboratory
Baltimore, Maryland

1 Rand Corporation
Attn: Dr. H.H. Bailey
1700 Main Street
Santa Monica, California

1 Massachusetts Institute of Technology
Servomechanisms Laboratory
Cambridge 39, Massachusetts

1 General Precision Laboratory, Inc.
63 Bedford Road
Pleasantville, New York

10 Commander
Armed Services Technical Information Agency
Arlington Hall Station
Arlington 12, Virginia

Copies

1 NASA
Anacostia Naval Station
Washington 25, D.C.
Attn: Paul A. Lantz
(Unclassified only)

1 Commander
Aeronautical Systems Division
Wright-Patterson Air Force Base, Ohio
Attn: WWZSH, Mr. Wm. P. Lee
(For Martin Aircraft Co.)